On the Performance of Multi-tier Heterogeneous Cellular Networks with Idle Mode Capability

Chuan Ma[*†], Ming Ding[†], He Chen[*], Zihuai Lin[*], Guoqiang Mao[†♯] and David López-Pérez[♠]

[*] School of Electrical and Information Engineering, University of Sydney, Australia

[†] Data61, CSIRO, Australia

[♯] School of Computing and Communications, University of Technology, Sydney, Australia

[♠] Nokia Bell Labs, Ireland

Email: {chuan.ma, he.chen, zihuai.lin}@sydney.edu.au, Ming.Ding@data61.csicro.au, g.mao@ieee.org, david.lopez-perez@nokia.com

Abstract—This paper studies the impact of the base station (BS) idle mode capability (IMC) on the network performance of multi-tier and dense heterogeneous cellular networks (HCNs). Different from most existing works that investigated network scenarios with an infinite number of user equipments (UEs), we consider a more practical setup with a finite number of UEs in our analysis. More specifically, we derive the probability of which BS tier a typical UE should associate to and the expression of the activated BS density in each tier. Based on such results, analytical expressions for the coverage probability and the area spectral efficiency (ASE) in each tier are also obtained. The impact of the IMC on the performance of all BS tiers is shown to be significant. In particular, there will be a surplus of BSs when the BS density in each tier exceeds the UE density, and the overall coverage probability as well as the ASE continuously increase when the BS IMC is applied. Such finding is distinctively different from that in existing work. Thus, our result sheds new light on the design and deployment of the future 5G HCNs.

I. INTRODUCTION

Commercial wireless networks are evolving towards higher frequency reuse by deploying smaller cells [1] to meet the explosively increasing demand for more mobile data traffic [2]. Heterogeneous cellular networks (HCNs), which are comprised of a conventional cellular network overlaid with a diverse set of small cell base stations (BSs), such as metro-, pico- and femto-cells, can help to realize such view and support much higher data rates per unit area than conventional networks. It is important to note that each BS tier in a HCN may have different characteristics, e.g., different spatial density, transmit power, path loss function, etc. A comprehensive analysis that takes into account the differences among different BS tiers in a HCN has been carried out in [3], where the BS locations are modeled as a homogeneous poison point process (HPPP). In [3], a flexible user equipment (UE) association strategy was considered, and each BS tier was assumed to have different spatial densities, transmit powers as well as path loss exponents.

The co-channel deployment of macro cell and small cell BSs in HCNs, i.e., all BS tiers operate on the same frequency spectrum, have attracted considerable attention recently, e.g., [4], [5]. Andrews *et al.* in [6] first analyzed the coverage probability of a single-tier small cell network by modeling BS locations as a HPPP. That study concluded that the coverage probability does not depend on the density of BSs in interference-limited scenarios (i.e., when the BSs are dense enough). Following [6], Jo *et al.* in [7] also reached the same conclusion for each BS tier in a multi-tier HCN. However, it is important to note that the aforementioned work assumed an unlimited number of UEs in the network, which implies that all BSs would always be active and transmit in all time and frequency resources. Obviously, this may not be the case in practice.

To attain a more practical network performance, Lee *et al.* in [8] first analyzed the coverage probability of a single-tier small cell network with a finite number of UEs, and derived an optimal BS density accordingly, by considering the tradeoff between the performance gain and the resultant network cost. Recently, Ding *et al.* in [9] analyzed the coverage probability and area spectral efficiency (ASE) of a single-tier small BS network with probabilistic line-of-sight (LoS) and non-LoS (NLoS) transmissions, in which the UE number is finite (e.g., 300 UEs/km^2) and the small cell BS has an idle mode capability (IMC). More specifically, if there is no active UE within the coverage areas of a certain BS, that BS will turn off its transmission module using the idle mode. The IMC switches off unused BSs, and thus can improve the network energy efficiency and the UEs' coverage probability as the network density increases. This is because UEs can receive stronger signals from the closer BSs, while the interference power remains constant thanks to the IMC. This conclusion in [9] - the coverage probability actually depends on the density of BSs in a interference-limited network - is fundamentally different from the previous results in [6] and [7], and presents new insights for the design of 5G networks. Furthermore, the IMC even changes the capacity scaling law in ultra-dense networks (UDN) [10].

However, the performance analysis presented in [8] and [9] is only applicable to the single-tier small cell networks. To our best knowledge, the theoretical study of multi-tier and dense HCNs with a finite number of users has not been conducted before, although some preliminary simulation results can be found in [1].

Motivated by the above theoretical gap, in this paper, we for the first time analyze the coverage probability and ASE of a HCN with *i)* multiple BS tiers, *ii)* an IMC at small cell

BSs, and *iii)* a limited number of UEs. To this end, we first derive an analytical expression for the density of active BSs in each tier. Based on this, the analytical expressions of the coverage probability and ASE for the HCNs with IMC are obtained. It is worth pointing out that the extension from a single-tier network scenario to a multi-tier one is *not* trivial, because BS activation needs to be considered for both the intra-tier and inter-tier BSs.

The rest of this paper is structured as follows. We describe the system model in Section II, and present the main analytical results on the activated BS density, the coverage probability and the ASE for each BS tier and for the overall HCN in Section III. Numerical results are discussed in Section IV. Finally, the conclusions are drawn in Section V.

II. SYSTEM MODEL

We consider a general HCN model consisting of M BS tiers that are characterized by different spatial densities and transmit powers. The positions of BSs in the i-th tier are modeled by a HPPP Φ_i with a density of λ_i BSs/km^2. The positions of UEs are also modeled according to a HPPP Φ_u with a density of λ_u UEs/km^2 that is independent of $\{\Phi_i\}_{i=1,\cdots,M}$. In the majority of the existing works, λ_u was assumed to be sufficiently large, so that each BS in each tier always has at least one associated UE. However, in our model with finite BS and UE densities, there may be no UE associated to a BS, and thus such BS will be turned off thanks to the IMC.

We consider a maximum average received power based cell association strategy, where each UE associates to only one BS that provides the maximum average received power. The average received power from the i-th tier is given by

$$S_i = P_i r^{-\alpha}, \qquad (1)$$

where P_i is the BS transmit power in the i-th tier, r is the distance between the BS and a typical UE sitting at the origin, and α is the path loss exponent.

In Fig. 1, we show an illustration of the proposed network, which consists of two BS tiers. In this case, UE 1 connects to BS 2 instead of BS 1 in tier 1 under the assumption that BS 2 provides the strongest average received signal. The other BSs are in idle mode since there is no UE associated to them.

Since UEs are randomly and uniformly distributed in the network, we adopt the following assumption: The activated BSs in each tier follow a HPPP distribution $\widetilde{\Phi}$, the density of which is denoted by $\widetilde{\lambda}_i$ BSs/km^2 [9], [11].

The SINR of the typical UE with a random distance r from its associated BS in the i-th tier is

$$\text{SINR}_i(r) = \frac{P_i h_{i0} r^{-\alpha}}{\sum_{j=1}^{M} \sum_{k \in \widetilde{\Phi} \backslash b_0} P_j h_{jk} |Y_{jk}|^{-\alpha} + \sigma^2}, \qquad (2)$$

where h_{i0} and h_{jk} is the exponentially distributed channel power with unit mean from the serving BS and the k-th interfering BS in the j-th tier (assuming Rayleigh fading), respectively, $|Y_{jk}|$ is the distance from the activated BS in the j-th tier to the origin, and b_0 is the serving BS in the i-th
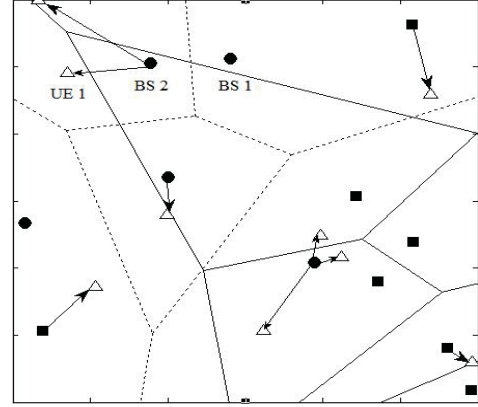

Fig. 1. Stochastic-geometry model of a two BS tier HCN. The tier 1 BSs, tier 2 BSs and UEs are marked with solid squares, solid dots and empty triangles, respectively. Each UE is connected to the BS that provides the strongest average receive signal, which is marked by a black arrow. BSs with no UE associated are in idle mode.

tier. Note that only the activated BSs in $\widetilde{\Phi} \backslash b_0$ inject effective interference into the network, since the other BSs are muted.

It is important to note that it has been shown in [12] that the analysis of the following factors/models is not urgent, as they do not change the qualitative conclusions of this type of performance analysis in UDNs: *(i)* a non-Poisson distributed BS density, *(ii)* a BS density dependent transmission power, *(iii)* a more accurate multi-path modeling with Rician fading, and *(iv)* an additional modeling of correlated shadow fading. Thus, we will concentrate on presenting our most fundamental discoveries in this paper, and show the minor impacts of the above factors/models in the journal version of this work.

III. ANALYTICAL RESULTS

To evaluate the impact of the IMC on the performance of each BS tier, we first analyze the probability of a given average number of UEs in each cell. Then, we derive expressions for the coverage probability and the ASE.

A. Average Number of UEs in each Cell

The coverage area of each small cell is a random variable V, representing the size of a Poisson Voronoi cell. Although there is no known closed-form expression for V's probability distribution function (PDF), some accurate estimates of this distribution have been proposed in the literature, e.g., [13] and [14].

In [13], a simple gamma distribution derived from Monte Carlo simulations was used to approximate the PDF of V for the BS in the i-th tier, given by

$$f_{V_i}(x) = (b\lambda_i)^q x^{q-1} \frac{\exp(-b\lambda_i x)}{\Gamma(q)}, \qquad (3)$$

where q and b are fixed values with $q = b = 3.5$, $\Gamma(x) = \int_0^{+\infty} t^{x-1} e^{-t} dt$ is the standard gamma function and λ_i is the BS density of the i-th tier.

Since the distribution of UEs follows a HPPP with a density of λ_u, given a Voronoi cell with size x, the number of

UEs located in this Voronoi cell is a Poisson random variable with a mean of $\lambda_u x$. Denoting by N_i the number of UEs located in a Voronoi cell in the i-th tier, we have

$$
\begin{aligned}
&\mathbb{P}[N_i = n] \\
&= \int_0^{+\infty} \frac{(\lambda_u x)^n}{n!} \exp(-\lambda_u x) f_{V_i}(x) dx \\
&\overset{(a)}{=} \frac{(b\lambda_i)^q (\lambda_u)^n}{n!\Gamma(q)(\lambda_u + b\lambda_i)^{q+n}} \int_0^{+\infty} \exp(-\xi)\xi^{n+q-1} d\xi \\
&\overset{(b)}{=} \frac{\Gamma(n+q)}{\Gamma(n+1)\Gamma(q)} \left(\frac{\lambda_u}{\lambda_u + b\lambda_i} \right)^n \left(\frac{b\lambda_i}{\lambda_u + b\lambda_i} \right)^q, \quad n \geq 0
\end{aligned}
\tag{4}
$$

where step (a) is obtained by using $\xi = (\lambda_u + b\lambda_i)x$, and step (b) is obtained by using the definition of the gamma function.

B. Probability of a UE associated to the i-th Tier

According to (1), each BS tier's density and transmit power determine the probability that a typical UE is associated with a BS in this tier. The following theorem provides the per-tier association probability, which is essential for deriving the main results in the sequel.

Theorem 1. *The probability of a typical UE associated with a BS in the i-th tier is given by:*

$$
A_i = \frac{\lambda_i}{\sum_{j=1}^{M} \lambda_j C_j{}^2},
\tag{5}
$$

where i denotes the index of the BS tier associating with the typical UE, and $C_j = (\frac{P_j}{P_i})^{\frac{1}{\alpha}}$, where P_i is the BS transmit power of the i-th tier, and α is its path loss exponent.

Proof. See Appendix A. □

The intuition of Theorem 1 is that a UE prefers to connect to the tier of BS with higher spatial density and transmit power, which follows the maximum received power based cell association strategy.

C. Density of activated BSs in the i-th tier

After attaining the probability of one UE associating to a BS in the i-th tier, we are ready to derive the density of activated BS in the i-th tier.

Defined by $\mathbb{P}_i^{\text{off}}(n)$ the probability that the BS are in the i-th tier is inactive when there are n UEs in its coverage, then $\mathbb{P}_i^{\text{off}}(n)$ is given by

$$
\mathbb{P}_i^{\text{off}}(n) = \mathbb{P}[N_i = n](1 - A_i)^n,
\tag{6}
$$

where $\mathbb{P}[N_i = n]$ is the probability that n UEs in a cell of i-th tier and has been obtained from (4), and A_i is the tier association probability obtained by Theorem 1.

Remark 1. *In (6), we assume there is no spatial correlation in the UE association process. Thus, selecting which BS to connect is assumed to be independent for different UEs. Hence, we have treated the association of the n UEs one*

by one. Note that this assumption may cause error as we underestimate the activated BS density of the considered BS tier. In the simulation section to be presented later, we will show that this error is negligible, especially when the density of BSs is large.

The density of activated BSs in the i-th tier $\widetilde{\lambda}_i$ can now be derived as

$$
\widetilde{\lambda}_i = \lambda_i \left(1 - \sum_{n=0}^{\infty} \mathbb{P}_i^{\text{off}}(n) \right),
\tag{7}
$$

where $\mathbb{P}_i^{\text{off}}(n)$ is the probability that the i-th tier is inactivated when there are n UEs in its coverage.

D. The Coverage Probability

We now investigate the coverage probability that the typical UE's SINR is above a predefined threshold τ. Since the typical UE is associated with at most one BS, the coverage probability is given by

$$
\mathbb{P}^{\text{cov}} = \sum_{i=1}^{M} A_i \mathbb{E}_r \left\{ \mathbb{P}[\text{SINR}_i(r) > \tau] \right\},
\tag{8}
$$

where A_i is the probability that the typical UE is associated with the BS in the i-th tier, which is given by (5) and $\mathbb{P}[\text{SINR}_i(r) > \tau]$ is the coverage probability of the typical UE associated with the BS in the i-th tier. Our main results on the coverage probability is presented in Theorem 2.

Theorem 2. *The coverage probability of a typical UE associated with the i-th tier is*

$$
\mathbb{E}_r \left\{ \mathbb{P}[\text{SINR}_i(r) > \tau] \right\}
$$

$$
= \int_0^{\infty} \exp \left\{ \frac{-\tau r^\alpha \sigma^2}{P_i} - \sum_{j=1}^{M} \left(\pi \widetilde{\lambda}_j C_j{}^2 r^2 Z(\tau, \alpha) \right) \right\} f_{r_i}(r) dr,
\tag{9}
$$

with $Z(\tau, \alpha) = \frac{2\tau}{\alpha - 2}{}_2F_1[1, 1 - \frac{2}{\alpha}; 2 - \frac{2}{\alpha}; -\tau]$, and $\alpha > 2$ and ${}_2F_1[\cdot]$ is the Gauss hypergeometric function.

Moreover, $f_{r_i}(r)$ is given by

$$
f_{r_i}(r) = \frac{2\pi\lambda_i r}{A_i} \exp \left(-\pi \sum_{j=1}^{M} \lambda_j C_j{}^2 r^2 \right).
\tag{10}
$$

Proof. Due to the page limitation, the proof will be relegated to the journal version of this paper. □

By substituting (5) and (9) into (8), we can obtain an analytical expression for the coverage probability. It is important to note that: *1)* The impact of the BS tier association and the BS selection on the coverage probability is measured in (5) and (10), the expressions of which are based on λ_i and λ_j. This is because all the BSs can be chosen by the UEs. *2)* The impact of the interference on the coverage probability is measured in (9). Note that instead of λ_j, we plug $\widetilde{\lambda}_j$ into (9), because only the activated BSs emit effective interference into the considered network.
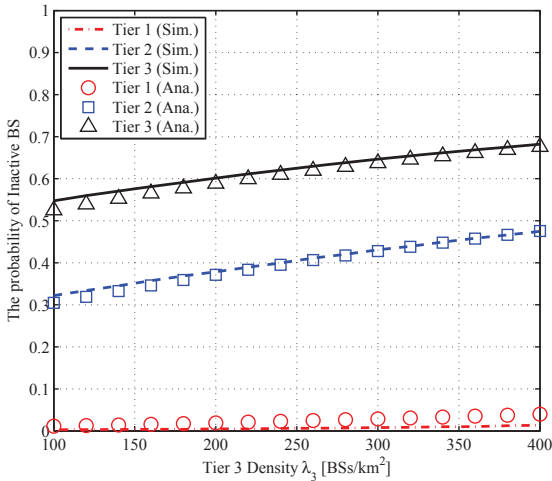
Fig. 2. The inactive BS probability for each HCN tier

Fig. 3. The coverage probability with respect to tier 2 density λ_2

E. Area Spectral Efficiency

In this subsection, we use the average ergodic rate of a typical UE randomly located in the considered multi-tier network to define the ASE. Using the same approach as in (8), the average ergodic rate can be expressed as

$$\mathbb{R} = \sum_{i=1}^{M} A_i \mathbb{R}_i, \qquad (11)$$

where $\mathbb{R}_i$ is the average ergodic rate of a typical UE associated with the i-th tier, and it is defined by

$$\mathbb{R}_i \triangleq \mathbb{E}_r \left\{ \mathbb{E}_{\text{SINR}_i} [\log_2(1 + \text{SINR}_i(r))] \right\}. \qquad (12)$$

The unit of the average rate is bps/Hz/km². It is important to note that the average is taken over both the channel fading distribution and the spatial PPP. The ergodic rate is first averaged on the condition that the typical UE is at a distance x from its serving BS in the i-th tier. Then, the rate is averaged by calculating the expectation over the distance r.

We present our results on $\mathbb{R}_i$ in Theorem 3 shown on the top of next page. By substituting (5) and (13) into (11), we then can obtain an analytical expression for the ASE.

IV. SIMULATION AND DISCUSSION

In this section, we evaluate the network performance and provide numerical results to validate the accuracy of our analysis.

A. Validation and Discussion on the BS Inactive Probability

We consider a 3-tier HCN defined by the 3GPP [15] to show the accuracy of our modeling. In particular, we use the following parameter values: $P_1 = 46$ dBm, $P_2 = 30$ dBm, $P_3 = 24$ dBm, $\lambda_1 = 10$ BSs/km², $\lambda_2 = 100$ BSs/km² and $\lambda_3 \in [100, 500]$ BSs/km². Besides, we adopt the following parameters for the network: $\alpha = 3.75$, $q = b = 3.5$, and the UE density is set to $\lambda_u = 300$ UEs/km². In Fig. 2, we
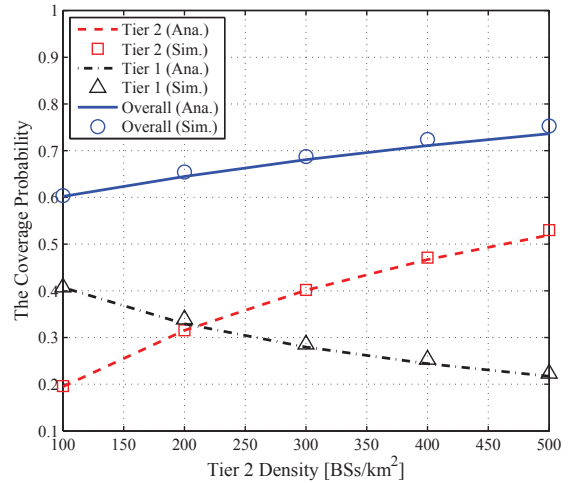
draw curves of $\mathbb{P}_i^{\text{off}}$ versus λ_3. As we can observe from this figure, our analytical results match well with the simulation results. Moreover, they also show that *i)* the probability of a BS being inactive in each tier increases with λ_3, when λ_u is a finite value, and that *ii)* the BSs with a lower transmit power have a less activation probability. For example, more than 40% and 60% of the BSs in tier 2 and tier 3 are idle when $\lambda_3 > 300$ BSs/km^2. This means that a large number of UEs are associated with the BSs in tier 1, as they can provide stronger signals to these UEs.

B. Validation and Discussion on the Coverage Probability

In this section, we first validate the accuracy of Theorem 2, where the network consists of 2 BS tiers. Specially, we use $P_1 = 30$ dBm, $P_2 = 24$ dBm, $\lambda_1 = 100$ BSs/km² and $\tau = 0$ dB. The rest of the parameters are the same as those in the previous subsection. In Fig. 3, we show the results of $\mathbb{P}^{\text{cov}}$ with respect to λ_1. As we can see from the figure, there are some small errors between the simulation and analytical results in each tier. For example, there is about 1% error when λ_2 is about 200 BSs/km². With the increasing number of BSs, the error becomes insignificant. The reason of such error is that the spatial correlation in UE association process is not considered in our analysis. Specially, when performing simulations, nearby UEs have a high probability of being covered and served by the same BS. However, for tractability, in the analysis, we consider the BS association of different UEs as independent process, which underestimates the active BS density. Due to the good accuracy of $\mathbb{P}^{\text{cov}}$, we will only use analytical results of $\mathbb{P}^{\text{cov}}$ for the figures in the sequel.

In Fig. 4, we compare our analytical results of coverage probability with those in [3]. In [3], an infinite number of UEs are considered, so all BSs are working in the fully-loaded mode. As can be observed from Fig. 4, based on the results in [3], the coverage probabilities of tier 1 and tier 2 decreases and increases as the network densifies,

Theorem 3. *The average ergodic rate of a typical UE associated with the BS in the i-th tier is*

$$\mathbb{R}_i = \frac{2\pi\lambda_i}{A_i} \int_0^\infty \int_0^\infty r \exp\left\{-(2^t-1)r^\alpha\sigma^2 P_i^{-1} - \pi r^2\left\{\sum_{j=1}^m C_j{}^2\left[\widetilde{\lambda}_j Z(2^t-1,\alpha)+\lambda_j\right]\right\}\right\} dt dr, \tag{13}$$

where $Z(e^t-1,\alpha) = \frac{2(2^t-1)}{\alpha-2}{}_2F_1[1,1-\frac{2}{\alpha};2-\frac{2}{\alpha};1-2^t]$, and $\alpha > 2$.

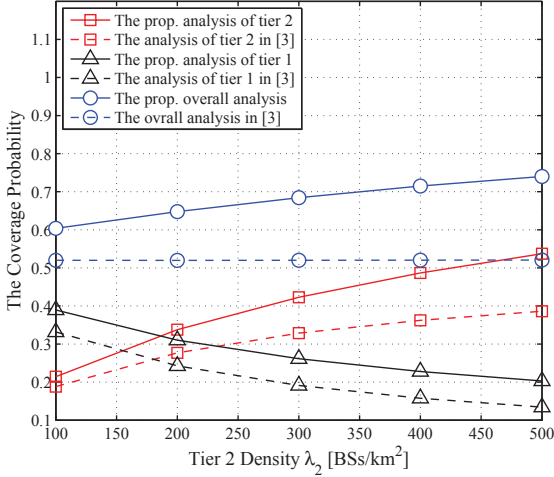*Proof.* Due to the page limitation, the proof will be relegated to the journal version of this paper. ☐

Fig. 4. The coverage probability compared with the analytical results in [3]

Fig. 5. The ASE with respect to tier 2 density λ_2

respectively. As a result, the overall coverage probability approaches a constant. However, our analytical results show that although the coverage probabilities of tier 1 and tier 2 show a similar trend as those in [3] (also decreases and increases as the network densifies), the overall coverage probability of the HCN does not follow the same trend. Due to the IMC considered in our analysis, the overall coverage probability performance continuously increases as the BS density increases. The intuition behind this phenomenon is that the interference power will remain constant with the network densification in each tier thanks to the IMC[1], while the signal power will continuously grow due to the closer proximity of the serving BS as well as the larger BS pool to select from. This enables stronger serving BS links.

C. Validation and Discussion on the ASE Performance

In this subsection, we validate the accuracy of Theorem 3, As in the previous subsection, the network consists of 2 BS

[1]The interference power will become constant eventually when there is an increasing number of BSs. Because of the IMC, the number of active BSs is at most equal to the number of UEs, and the distance between one UE and its serving BS keeps decreasing. Thus, from the point of the typical UE, the injecting interference from other active BSs can be regarded as the aggregate interference generated by BSs on a HPPP plane with the same intensity as the UE intensity. Such aggregate interference is bounded and statistically stable [6].
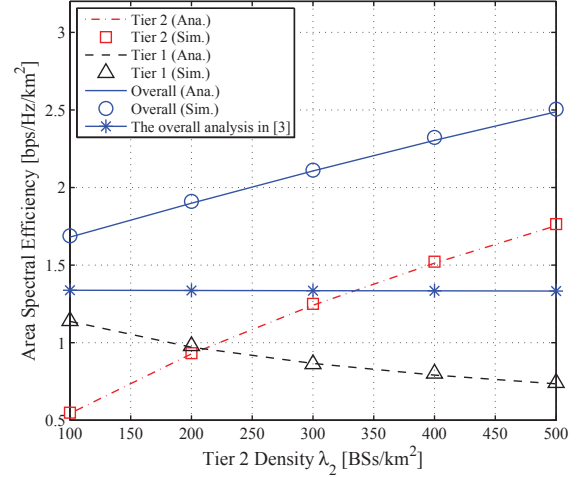
tiers, and other parameters are set to be the same with the previous subsections.

In Fig. 5, we can observe that the ASE analytical results match well with the simulation results. Moreover, the results show that with the increasing number of tier 2 BSs, the ASE of tier 2 increases, while that of tier 1 reduces. The performance improvement of tier 2 is because the interference power from tier 2 BSs remains constant thank to the IMC, while the UE is served by a stronger link using a BS in the tier 2, as the network densifies. However, for the UE associated with tier 1, although the power of the serving link does not decline, the cross-tier interference power from tier 2 BSs keeps increasing. Thus, the performance of tier 1 shows a decreasing trend. We also compare our proposed overall results with those in [3]. Different from [3], the impact of IMC is considered in our proposed model, which results in a better system performance. The performance of our proposed model grows with the BS density, while that in [3] is kept constant as the number of BSs increases. This new observation sheds new light on the design and deployment of HCNs in 5G.

V. Conclusions

In this paper, we have studied the impact of the IMC on the network performance in multi-tier HCNs with a

limited number of UEs. It is interesting to observe that the number of tiers and density of BSs do affect the cell activation/inactivation probability, the coverage probability and the ASE. Different from the existing works, our results imply that densifying the BSs in each tier will increase the network capacity as well as the quality of service for UEs.

In the considered network model, UEs tend to connect to BSs with a larger transmit power, e.g., the macrocell BSs, and this effect will be aggravated as the power difference among different tiers of BSs becomes larger. Thus, this leads to a high small cell inactivation probability and an over-utilization of macrocells. To avoid this phenomenon, the current 4G LTE networks have adopted the technologies of cell range expansion (CRE) and enhanced inter-cell interference coordination (eICIC) combined with the almost blank subframe (ABS) mechanism [1]. As our future work, we will consider such mechanisms in our theoretical analysis.

APPENDIX A
PROOF OF THEOREM 1

When the typical UE is associated with a BS in the i-th tier, the received signal from the serving BS is the largest one, which can be interpreted as:

$$S_{i,0} > \max_{j,j\neq i} S_{j,0} \Longrightarrow \begin{cases} S_{i,0} > S_{1,0} \\ S_{i,0} > S_{2,0} \\ ... \\ S_{i,0} > S_{j,0} \end{cases} \Longrightarrow \begin{cases} r_{1,0} > C_2 r_{i,0} \\ r_{2,0} > C_3 r_{i,0} \\ ... \\ r_{j,0} > C_j r_{i,0}, \end{cases} \tag{14}$$

where $C_j = \left(\frac{P_j}{P_i}\right)^{\frac{1}{\alpha}}$, $i = 2, 3, ..., m$.

We can calculate the probability of the event in (14) as

$$\mathbb{P}\left(S_{i,0} > \max_{j,j\neq i} S_{j,0}\right) = \prod_{j=1,j\neq i}^{M} \mathbb{P}\left(r_{j,0} > C_j r_{i,0}\right)$$

$$= \prod_{j=1,j\neq i}^{M} \mathbb{P}[\text{No BS closer than } C_j r_{i,0} \text{ in the } j\text{-th tier}]$$

$$= \prod_{j=1,j\neq i}^{M} \exp(-\pi\lambda_j C_j{}^2 r_{i,0}^2). \tag{15}$$

According to the null probability of a 2-D Poisson process with density λ_i, the PDF of $r_{i,0}$ is given by

$$\mho_{r_{i,0}}(r) = \exp(-\pi\lambda_i r^2)2\pi\lambda_i r. \tag{16}$$

By combining (15) and (16) together, we then have

$$A_i = \mathbb{E}_{r_{i,0}}\left\{\mathbb{P}\left(S_{i,0} > \max_{j,j\neq i} S_{j,0}\right)\right\}$$

$$= \int_0^\infty \prod_{j=1,j\neq i}^{M} \exp(-\pi\lambda_j C_j{}^2 r^2)\mho_{r_{i,0}}(r)dr$$

$$= \frac{\lambda_i}{\sum\limits_{j=1}^{M} \lambda_j C_j{}^2}. \tag{17}$$

REFERENCES

[1] D. López-Pérez, M. Ding, H. Claussen, and A. H. Jafari, "Towards 1 gbps/ue in cellular systems: Understanding ultra-dense small cell deployments," *IEEE Communications Surveys & Tutorials*, vol. 17, no. 4, pp. 2078–2101, 2015.

[2] Cisco, "Visual networking index forecast, 2015–2020," 2015.

[3] H.-S. Jo, Y. J. Sang, P. Xia, and J. G. Andrews, "Heterogeneous cellular networks with flexible cell association: A comprehensive downlink sinr analysis," *IEEE Transactions on Wireless Communications*, vol. 11, no. 10, pp. 3484–3495, 2012.

[4] Q. Ye, B. Rong, Y. Chen, M. Al-Shalash, C. Caramanis, and J. G. Andrews, "User association for load balancing in heterogeneous cellular networks," *IEEE Transactions on Wireless Communications*, vol. 12, no. 6, pp. 2706–2716, June 2013.

[5] Z. Gao, L. Dai, D. Mi, Z. Wang, M. A. Imran, and M. Z. Shakir, "Mmwave massive-mimo-based wireless backhaul for the 5g ultra-dense network," *IEEE Transactions on Wireless Communications*, vol. 22, no. 5, pp. 13–21, October 2015.

[6] J. G. Andrews, F. Baccelli, and R. K. Ganti, "A tractable approach to coverage and rate in cellular networks," *IEEE Transactions on Communications*, vol. 59, no. 11, pp. 3122–3134, 2011.

[7] H. S. Dhillon, R. K. Ganti, F. Baccelli, and J. G. Andrews, "Modeling and analysis of k-tier downlink heterogeneous cellular networks," *IEEE Journal on Selected Areas in Communications*, vol. 30, no. 3, pp. 550–560, April 2012.

[8] S. Lee and K. Huang, "Coverage and economy of cellular networks with many base stations," *IEEE Communications Letters*, vol. 16, no. 7, pp. 1038–1040, 2012.

[9] M. Ding, D. L. Pérez, G. Mao, and Z. Lin, "Study on the idle mode capability with los and nlos transmissions," *arXiv preprint arXiv:1608.06694*, 2016.

[10] M. Ding, D. Lpez-Prez, and G. Mao, "A new capacity scaling law in ultra-dense networks," *arXiv:1704.00399 [cs.NI]*, Apr. 2017. [Online]. Available: https://arxiv.org/abs/1704.00399

[11] C. Yang, Y. Yao, Z. Chen, and B. Xia, "Analysis on cache-enabled wireless heterogeneous networks," *IEEE Transactions on Wireless Communications*, vol. 15, no. 1, pp. 131–145, 2016.

[12] M. Ding and D. Lpez-Prez, "On the performance of practical ultra-dense networks: The major and minor factors," *The IEEE Workshop on Spatial Stochastic Models for Wireless Networks (SpaSWiN) 2017*, pp. 1–8, May 2017. [Online]. Available: https://arxiv.org/abs/1701.07964

[13] J.-S. Ferenc and Z. Néda, "On the size distribution of poisson voronoi cells," *Physica A: Statistical Mechanics and its Applications*, vol. 385, no. 2, pp. 518–526, 2007.

[14] A. Hinde and R. Miles, "Monte carlo estimates of the distributions of the random polygons of the voronoi tessellation with respect to a poisson process," *Journal of Statistical Computation and Simulation*, vol. 10, no. 3-4, pp. 205–223, 1980.

[15] 3GPP, "TR 36.828: Further enhancements to LTE Time Division Duplex (TDD) for Downlink-Uplink (DL-UL) interference managemnet and traffic adapataion," June 2012.